

## Lateral tunneling through the controlled barrier between edge channels in a two-dimensional electron system

A. A. Shashkin, V. T. Dolgoplov, and E. V. Deviatov

*Institute of Solid State Physics, Russian Academy of Sciences, 142432 Chernogolovka, Moscow Region, Russia*

B. Irmer, A. G. C. Haubrich, and J. P. Kotthaus

*Ludwig-Maximilians-Universität, D-80539 München, Germany*

M. Bichler and W. Wegscheider

*Walter Schottky Institut, Technische Universität München, D-85748 Garching, Germany*

(Submitted 18 March 1999)

Pis'ma Zh. Éksp. Teor. Fiz. **69**, No. 8, 561–566 (25 April 1999)

A study is made of the lateral tunneling between edge channels at the depletion-induced edges of a gated two-dimensional electron system, through a gate-voltage-controlled barrier arising when the donor layer of the heterostructure is partly removed along a fine strip by means of an atomic force microscope. For a sufficiently high barrier the typical current–voltage characteristic is found to be strongly asymmetric, having, in addition to the positive tunneling branch, a negative branch that corresponds to the current overflowing the barrier. It is established that the barrier height depends linearly on both the gate voltage and the magnetic field, and the data are described in terms of electron tunneling between the outermost edge channels. © 1999 American Institute of Physics. [S0021-3640(99)00708-2]

PACS numbers: 73.40.Gk, 73.40.Hm

Recently there has arisen much interest in lateral tunneling to the edge of a two-dimensional electron system (2DES), which is related not only to the problem of integer and fractional edge states in the 2DES but also to that of resonant tunneling and Coulomb blockade.<sup>1–7</sup> The tunneling regime was identified by the presence of exponential dependences of the measured current on either source–drain voltage<sup>1–4</sup> or magnetic field.<sup>5</sup> For producing a tunnel barrier a number of methods were used: (i) gate voltage depletion of a narrow region inside the 2DES;<sup>1–4,7</sup> (ii) focused-ion-beam insulation writing;<sup>6</sup> (iii) cleaved-edge overgrowth technique.<sup>5</sup> Insofar as the tunnel barrier parameters are not well-controllable values, it is important for using the first method that one can tune the barrier on the same sample. In contrast to vertical tunneling into the bulk of the 2DES in a quantizing magnetic field, when the 2DES spectrum is manifested,<sup>8,9</sup> in lateral tunneling the electrons can always tunnel to Landau levels that bend up at the edge to form edge channels where they intersect the Fermi level, i.e., the spectrum gaps are not seen directly in lateral tunneling. Instead, it reflects the edge channel structure and density of states. For both the integer and fractional quantum Hall effect, a power-law behavior of

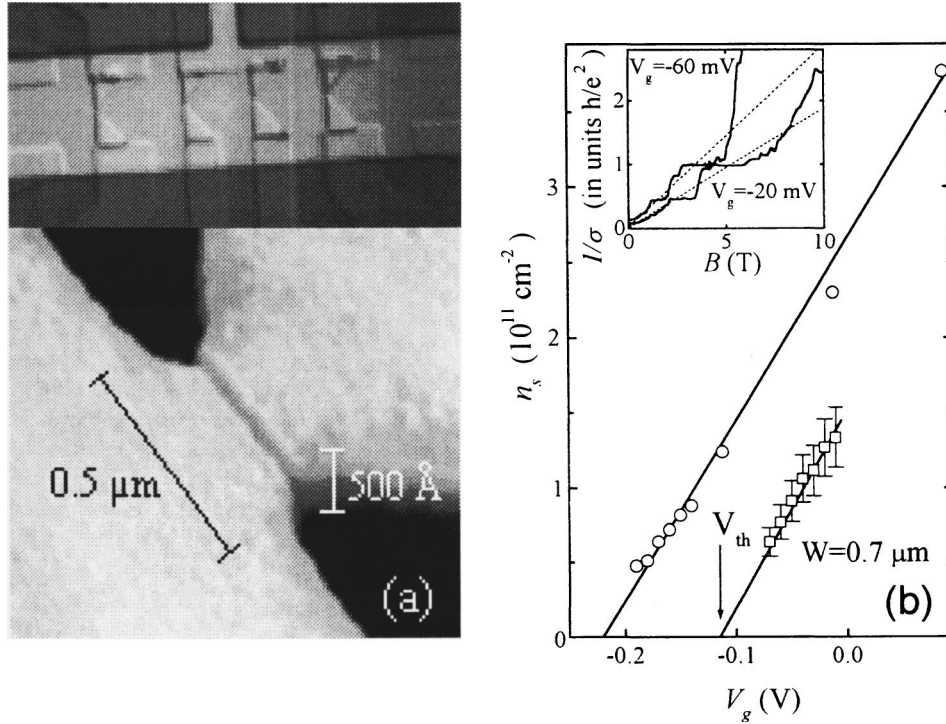


FIG. 1. (a) Top view on the sample (top), and a blowup of one of the constrictions after etching of the oxidized part of the mesa as performed solely for visualization purposes (bottom). (b) Gate voltage dependences of the electron density in the oxidized (squares) and unoxidized (circles) regions of the 2DES. An example of the magnetoconductance in the barrier region is shown in the inset. The value of  $n_s$  is extracted from the slope of the dashed lines with 10% uncertainty.

the density of states at the 2DES edge is expected. Since this can interfere with the barrier distortion at electric fields in the nonlinear response regime, the results of lateral tunneling experiments obtained from measurements of the current–voltage curves<sup>5</sup> should be treated with care.

Here we investigate the lateral tunneling in narrow constrictions in which, along a thin strip across, the donor layer of a GaAs/AlGaAs heterostructure is partly removed using an atomic force microscope (AFM). A controlled tunnel barrier is created by gate depletion of the whole of the sample. The well-developed tunneling regime is indicated by strongly asymmetric diodelike current–voltage characteristics of the constriction, which are sensitive to both the gate voltage  $V_g$  and the normal magnetic field  $B$ . The behavior of the tunneling part of the current–voltage curves points to electron tunneling between the outermost edge channels.

The samples are triangular constrictions of a 2D electron layer with different widths  $W=0.7, 0.4, 0.3,$  and  $0.2 \mu\text{m}$  of the thinnest part; see Fig. 1a. These are made using standard optical and electron beam lithography from a wafer of GaAs/AlGaAs heterostructure with a low-temperature mobility  $\mu=1.6 \times 10^6 \text{ cm}^2/\text{Vs}$  and a carrier density  $n_s=4 \times 10^{11} \text{ cm}^{-2}$ . Within each constriction the donor layer is removed along a fine line

by locally oxidizing the heterostructure using AFM induced oxidation.<sup>10</sup> This technique allows one to define 140 Å wide oxide lines of sufficient depth and oxide quality so as to partly remove the donor layer and, therefore, locally decrease the original electron density. The whole structure is covered with a metallic gate, which enables us to tune the carrier density everywhere in the sample. As the 2D layer is depleted, the oxidized regions get depopulated first, resulting in the creation of tunnel barriers. Potential probes are made to the sample to permit transport measurements.

For the measurements we apply a dc voltage,  $V_{sd}$ , between the source (grounded) and drain contacts of one of the constrictions, modulated with small ac voltage with amplitude  $V_{ac}=40 \mu\text{V}$  and frequency  $f=20 \text{ Hz}$ . A gate voltage is applied between the source and the gate. We measure the real part of the ac current, which is proportional to the differential conductance  $dI/dV$ , as a function of bias voltage  $V_{sd}$  ( $I$ - $V$  characteristics) using a home-made  $I$ - $V$  converter and a standard lock-in technique. The behavior of the  $I$ - $V$  characteristics is investigated as a function of both the gate voltage and magnetic field. The measurements are performed at a temperature of about 30 mK in magnetic fields of up to 14 T. The results obtained on different constrictions are qualitatively similar.

To characterize the sample we extract the gate-voltage dependence of the electron density from the behavior of magnetoconductance plateaus in the barrier region and in the rest of the 2DES (Fig. 1b). The analysis is made at high fields, where the size-quantization-caused effect of conductance plateaus in narrow constrictions is dominated by magnetic field quantization effects.<sup>11</sup> As is seen from Fig. 1b, if the barrier region is depopulated ( $V_g < V_{th}$ ), the electron density in the surrounding areas is still high enough to provide good conduction. The slopes of the curves  $n_s(V_g)$  in the oxidized region and in the rest of the 2DES turn out to be equal within our accuracy. The distance between the gate and the 2DES is determined to be  $d \approx 570 \text{ Å}$ ; as the corresponding growth parameter is about 400 Å, the 2D layer thickness contributes appreciably to the distance  $d$ . We have found that even in the unoxidized region the electron density at  $V_g=0$  can be different after different coolings of the sample on account of slight threshold shifts: it falls within the range  $2.5 \times 10^{11}$  to  $4 \times 10^{11} \text{ cm}^{-2}$  and is always higher than in the barrier region.

The typical  $I$ - $V$  characteristic of the constriction in the well-developed tunneling regime is strongly asymmetric and includes an overflowing branch at  $V_{sd} < 0$  and the tunneling branch at  $V_{sd} > 0$ ; see Fig. 2a. The tunneling branch is much smaller and saturates rapidly in zero  $B$  with increasing bias voltage. The onset voltages  $V_O$  and  $V_T$  for these branches are defined in a standard way as shown in the figure. The tunneling regime can be attained both by decreasing the gate voltage and by increasing the magnetic field, as is evident from Fig. 2a. We have checked that the shape of  $I$ - $V$  characteristics is not influenced by interchanging the source and drain contacts. Hence, the tunnel barrier is symmetric, and the asymmetry observed is not related to the constriction geometry.

To understand the origin of the asymmetry, let us consider a gated 2DES containing a potential barrier of approximately rectangular shape, with width  $L \gg d$ , in zero magnetic field. The 2D band bottom in the barrier region coincides with the Fermi level  $E_F$  of the 2DES at  $V_g$  equal to the threshold voltage  $V_{th}$ . Since in the barrier region for  $V_g < V_{th}$  an incremental electric field is not screened, the 2D band bottom follows the gate potential, so that the barrier height is equal to  $-e\Delta V_g = e(V_{th} - V_g)$ , where  $-e$  is the charge of an electron (Fig. 2b). Applying a bias voltage  $V_{sd}$  shifts the Fermi level in the drain contact

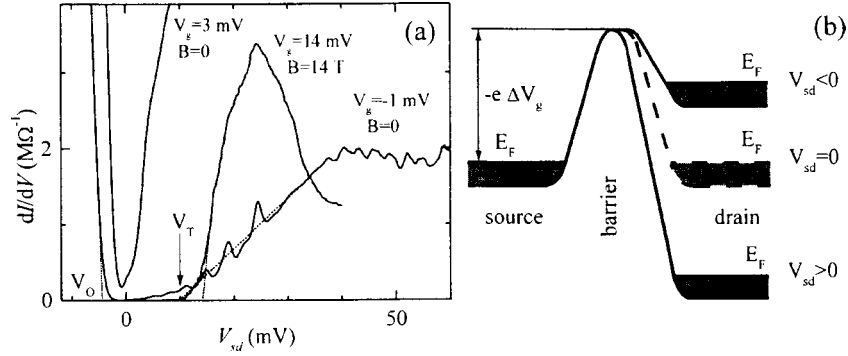


FIG. 2. (a)  $I$ - $V$  curves at different gate voltages and magnetic fields. The cases  $B=0$  and  $B \neq 0$  correspond to two coolings of the sample as compared in Fig. 3a.  $W=0.4 \mu\text{m}$ . (b) A sketch of the 2D band bottom in the barrier region for different source-drain biases  $V_{sd}$ .

by  $-eV_{sd}$ . Because of gate screening the voltage  $V_{sd}$  drops over a distance scale of the order of  $d$  near the boundary between the barrier and drain, and so the barrier height on the source side remains practically unchanged; see Fig. 2b. If  $V_{sd}$  reaches the onset voltage  $V_O = \Delta V_g$ , the barrier on the drain side vanishes, and electrons start to overflow from the drain to the source. In contrast, for  $V_{sd} > 0$  only the electron tunneling through the barrier from the source to the drain is possible. As  $V_{sd}$  increases above  $-\Delta V_g$ , the tunneling distance diminishes and the barrier shape becomes close to triangular. Within the triangular barrier approximation, in the quasiclassical limit of small tunneling probabilities, it is easy to deduce that the derivative of the tunneling current with respect to the bias voltage is expressed by the relation

$$\frac{dI}{dV} = \sigma_0 \exp\left(-\frac{4(2m)^{1/2}(-e\Delta V_g)^{3/2}L}{3\hbar eV_{sd}}\right) \ll \sigma_0, \quad (1)$$

where  $\sigma_0 \approx -(e^2/h)\Delta V_g W/V_{sd}\lambda_F$ ,  $m=0.067m_0$  ( $m_0$  is the free electron mass), and  $\lambda_F$  is the Fermi wavelength in the source. Obviously, the tunneling current is dominated by electrons in the vicinity of the Fermi level, and the tunneling distance  $L_T = -\Delta V_g L/V_{sd}$  should satisfy the inequality  $d \ll L_T < L$ . In accordance with Eq. (1), the expected dependence of the tunneling onset voltage  $V_T$  on gate voltage is given by  $V_T \propto (-\Delta V_g)^{3/2}$ .

As is seen from Fig. 3a, the expected behavior of both  $V_O$  and  $V_T$  with changing  $V_g$  does indeed occur. The dependences  $V_O(V_g)$  and  $V_T^{2/3}(V_g)$  are both linear; the slope of the former is very close to one. Extensions of these straight lines intercept the  $V_g$  axis at slightly different voltages, which points out that the triangular barrier approximation is good. The threshold voltage  $V_{th}$  for the generation of a 2DES in the barrier region, which is defined as a point of vanishing  $V_O$  (Fig. 3a), is coincident, within experimental uncertainty, with the value of  $V_{th}$  determined from the analysis of magnetoconductance plateaus (Fig. 1b).

A fitting of the set of  $I$ - $V$  characteristics at different  $V_g$  by Eq. (1) with parameters  $L$ ,  $V_{th}$ , and  $\sigma_0$  is depicted in Fig. 3b. The dependence of  $\sigma_0$  on  $\Delta V_g$  and  $V_{sd}$  is ignored against the background of the strong exponential dependence of  $dI/dV$ . Although three

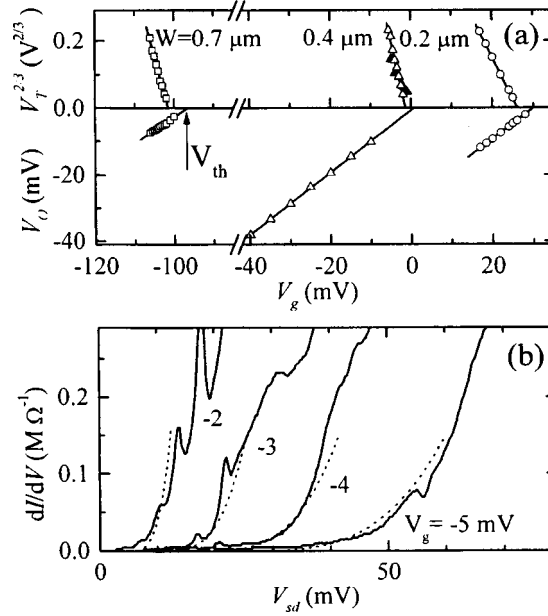


FIG. 3. (a) Change of the onset voltages  $V_O$  and  $V_T$  as defined in Fig. 2a with  $V_g$  at  $B=0$ ; and (b) the fit (dashed lines) of the  $I-V$  curves (solid lines) by Eq. (1) with the parameters  $L=0.6 \mu\text{m}$ ,  $\sigma_0=38 M\Omega^{-1}$ ,  $V_{th}=-0.4 \text{ mV}$ ;  $W=0.4 \mu\text{m}$ . In case (a), the data marked by filled triangles are obtained for the same cooling of the sample as the data at  $B=0$  in Fig. 2a and in case (b), whereas the open triangles correspond to the  $B \neq 0$  data of Figs. 2a and 4 as measured for the other cooling.

parameters are varied, the fit is very sensitive, except for  $\sigma_0$ , to their variation because of the exponential behavior of the  $I-V$  characteristics. One can see from Fig. 3b that the above model describes well the experiment at zero magnetic field. As expected, the determined parameter  $L=0.6 \mu\text{m}$  is much larger than  $d$ , i.e., the barrier shape at  $V_{sd}=0$  is approximately rectangular, and the value of  $V_{th}$  is close to the point where  $V_O$  (and  $V_T$ ) tends to zero (Fig. 3a). Similar results are obtained at the other two constrictions. In addition, we find that the coefficient  $\sigma_0$  for different constrictions does not scale with the constriction width  $W$ . This probably implies that the tunnel barriers, even with submicron lengths, are still inhomogeneous, which, however, does not seem crucial for the case of exponential  $I-V$  dependences.

Having tested that we are dealing with a controlled tunnel barrier, we investigate the tunneling in a normal magnetic field that gives rise to an emerging tunnel barrier in a manner similar to gate depletion (Fig. 2a). At a constant  $V_g > V_{th}$ , where there is no tunnel barrier in zero  $B$ , the magnetoconductance  $\sigma$  obeys a  $1/B$  law at weak fields and drops exponentially with  $B$  in the high-field limit, signaling the tunneling regime. Figure 4a presents the magnetic field dependence of the onset voltage  $V_O$ , which determines the barrier height. It is seen from the figure that the change of the barrier height  $-eV_O$  with  $B$  is very close to  $\hbar\omega_c/2$ , which points to a shift of the 2D band bottom by one-half of the cyclotron energy.

For describing the tunneling branch of the  $I-V$  characteristics we calculate the

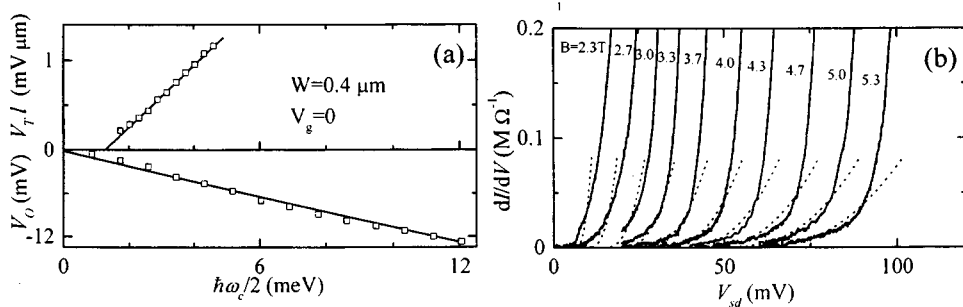


FIG. 4. (a) Behavior of the onset voltages  $V_O$  and  $V_T$  with magnetic field; and (b) the fit (dashed lines) of the  $I$ - $V$  curves (solid lines) by Eq. (4) with the parameters  $L=0.6 \mu\text{m}$ ,  $\sigma_0=1.3 \text{M}\Omega^{-1}$ , and  $V_{\text{th}}=-1.4 \text{mV}$ ;  $W=0.4 \mu\text{m}$ ,  $V_g=0$ .

tunneling probability in the presence of a magnetic field. This is not so trivial as at  $B=0$  because electrons tunnel through the magnetic parabola between edge channels at the induced edges of the 2DES. In the triangular barrier approximation one has to solve the Schrödinger equation with the barrier potential

$$U(x) = \frac{\hbar \omega_c}{2l^2} (x - x_0)^2 - eV_{\text{sd}} \frac{x}{L} - e\Delta V_g, \quad 0 < x < L, \quad (2)$$

where  $\omega_c$  is the cyclotron frequency,  $l$  is the magnetic length, and  $eV_{\text{sd}}$  is larger than the barrier height in the magnetic field. An electron at the Fermi level in the source tunnels through  $U(x)$  from the origin to a state with orbit center  $x_0$  such that  $0 < x_0 < L$ . If the barrier potential is dominated by the magnetic parabola (i.e., the magnetic length is the shortest), the problem reduces to the known problem of finding the energy levels in the shifted parabolic potential as caused by the linear term in Eq. (2). The value of  $x_0$  is determined from the condition of coincidence of a Landau level in the potential  $U(x)$  with the Fermi level in the source. If only the lowest Landau level is taken into consideration and the spin splitting is ignored, we get the minimum tunneling distance to the outermost edge channel in the drain:

$$x_0 = L_T = \frac{l}{2} \left( \frac{\hbar \omega_c L}{eV_{\text{sd}} l} - \frac{2\Delta V_g L}{V_{\text{sd}} l} - \frac{eV_{\text{sd}} l}{\hbar \omega_c L} \right) \gg d. \quad (3)$$

The first term in brackets in Eq. (3), which is dominant, is large compared to unity. Knowing the wave function of the lowest Landau level in the potential  $U(x)$  and neglecting the last term in Eq. (3), we obtain for the shape of the  $I$ - $V$  characteristics near the onset, where the tunneling probability is small,

$$\frac{dI}{dV} = \sigma_B \exp \left( - \frac{(\hbar \omega_c / 2 - e\Delta V_g)^2 L^2}{e^2 V_{\text{sd}}^2 l^2} \right) \ll \sigma_B. \quad (4)$$

Here  $\sigma_B$  is a prefactor which can be tentatively expected to be of the same order of magnitude as  $\sigma_0$ . From Eq. (4) it follows that at sufficiently strong magnetic fields the tunneling onset voltage  $V_T$  is related to the barrier height as  $V_T l \propto \hbar \omega_c / 2 - e\Delta V_g$ , which is consistent with the experiment (Fig. 4a). The solution (4) includes the case  $e\Delta V_g > 0$ ,

when a tunnel barrier is absent at zero magnetic field but arises with increasing  $B$ . This occurs apparently because of depopulation of the barrier region in the extreme quantum limit of magnetic field.

Figure 4b displays the fit of the  $I$ - $V$  characteristics at different magnetic fields by Eq. (4) with the parameters  $L$ ,  $V_{\text{th}}$ , and  $\sigma_B$ . The optimum values of  $L=0.6 \mu\text{m}$  and  $V_{\text{th}}=-1.5 \text{ mV}$  are found to be very close to the ones for the  $B=0$  case as determined for the same range of barrier heights; see Fig. 3b. Although this fact supports our considerations, they are not rigorous enough to permit discussing the considerable discrepancy between the preexponential factors with and without magnetic field.

The observed behavior of the  $I$ - $V$  characteristics with magnetic field in the transient region where their asymmetry is not yet strong (Fig. 2a) is similar to that of Refs. 4 and 5. Over this region, which is next to the region of exponential  $I$ - $V$  dependences at higher magnetic-field-induced tunnel barriers, our  $I$ - $V$  curves are close to power-law dependences, as was discussed in Ref. 5. There is little doubt that it is very difficult to analyze and interpret such  $I$ - $V$  curves without solving the tunneling problem rigorously. We note that the peak structures on the tunneling branch of the  $I$ - $V$  characteristics (see Figs. 2a and 3b) persist at relatively low magnetic fields and are very similar to those studied in Ref. 4. These may be hint at resonant tunneling through impurity states below the 2D band bottom.

This work was supported in part by the Russian Fund for Fundamental Research under Grants 97-02-16829 and 98-02-16632, the Program "Nanostructures" from the Russian Ministry of Sciences under Grant 97-1024, and the Volkswagen-Stiftung under Grant I/68769.

<sup>1</sup>A. Palevski, M. Heiblum, C. P. Umbach *et al.*, Phys. Rev. Lett. **62**, 1776 (1989).

<sup>2</sup>K. Ismail, D. A. Antoniadis, and H. I. Smith, Appl. Phys. Lett. **55**, 589 (1989).

<sup>3</sup>S. J. Manion, L. D. Bell, W. J. Kaiser *et al.*, Appl. Phys. Lett. **59**, 213 (1991).

<sup>4</sup>A. J. Peck, S. J. Bending, J. Weis *et al.*, Phys. Rev. B **51**, 4711 (1995).

<sup>5</sup>A. M. Chang, L. N. Pfeiffer, and K. W. West, Phys. Rev. Lett. **77**, 2538 (1996); M. Grayson, D. C. Tsui, L. N. Pfeiffer *et al.*, Phys. Rev. Lett. **80**, 1062 (1998).

<sup>6</sup>T. Bever, A. D. Wieck, K. von Klitzing, and K. Ploog, Phys. Rev. B **44**, 3424 (1991); T. Bever, A. D. Wieck, K. von Klitzing *et al.*, Phys. Rev. B **44**, 6507 (1991).

<sup>7</sup>T. Heinzel, D. A. Wharam, J. P. Kotthaus *et al.*, Phys. Rev. B **50**, 15113 (1994).

<sup>8</sup>J. P. Eisenstein, L. N. Pfeiffer, and K. W. West, Phys. Rev. B **50**, 1760 (1994).

<sup>9</sup>V. T. Dolgoplov, A. A. Shashkin, A. V. Aristov *et al.*, Phys. Rev. Lett. **79**, 729 (1997).

<sup>10</sup>B. Irmer, M. Kehrle, H. Lorenz, and J. P. Kotthaus, Appl. Phys. Lett. **71**, 1733 (1997).

<sup>11</sup>B. J. van Wees, L. P. Kouwenhoven, H. van Houten *et al.*, Phys. Rev. B **38**, 3625 (1988).